THERMAL BUOYANCY ON VENUS: UNDERTHRUSTING VS SUBDUCTION

Jeffrey D. Burt and James W. Head

Department of Geological Sciences, Brown University

Abstract In an effort to define the conditions distinguishing underthrusting and subduction in the Venus environment, we have modeled the thermal and buoyancy consequences of the subduction endmember. Predictions of the thermal evolution of a slab subducting at a fixed angle into the Venusian mantle are used to find slab densities based on slab composition and changes of temperature, pressure, and phase. The sustainability of subduction is assessed by considering the effects of slab buoyancy and mantle flow on the subduction angle. Mantle flow induced by slab motion applies torques on the slab, which are compared to buoyancy torques. Flow torques tend to decrease the angle of subduction. Buoyancy torques also act to decrease the subduction angle when the slab is positively buoyant. The basalt-eclogite phase transition dominates the transformation of positively buoyant slabs to negative buoyancy. Slabs that have descended to depths less than about 275 km remain positively buoyant. Beyond 275 km slabs become negatively buoyant. We predict that the combination of flow and buoyancy torques will tend to force initially subducted slabs to assume an underthrusting position, leading to crustal thickening, deformation, melting, and volcanism. This may provide a model explaining the association of compressional mountain belts and tessera blocks with apparent flexural rises, foredeeps, and voluminous volcanic deposits. Only special circumstances appear capable of promoting the conditions for negative slab buoyancy. These might include one where an underthrust slab becomes attached to or included in a densified crustal root created in a zone of crustal thickening. The subsequent delamination and sinking of the root may then lead to the subduction of the slab.

Introduction

Enhanced surface temperatures and a thinner lithosphere on Venus relative to Earth have been cited as contributing to increased lithospheric buoyancy. This would limit [Phillips and Malin, 1982], or prevent [Anderson, 1981] subduction on Venus, and favor the construction of thickened crust through underthrusting. Underthrusting may contribute to the formation of a number of features on Venus. For example, Freyja Montes, an east-west trending linear mountain belt in northern Ishtar Terra, lies south of a high plateau of complexly deformed terrain, Itzpapalotl Tessera, that contains evidence of extensive volcanic activity [Burt and Head, 1990]. Itzpapalotl is bounded to the north by Uorsar Rupes, a steep scarp marking a descent of 2 to 3 km elevation to a volcanic plains-filled foredeep. Further north are an outboard rise and the north polar plains of Venus. Freyja Montes is interpreted as an orogenic belt [Crumpler et al., 1986] and the region a zone of convergence and underthrusting of the north polar plains beneath Ishtar Terra, with consequent crustal thickening [Head, 1990].

Paper number 92GL01702
0094-8534/92/92GL-01702$03.00

Models for the formation of such mountain belts and associated features must explain compressional deformation, crustal thickening, and melt production.

While Venus lacks clear evidence of Earth-like plate tectonics, features resembling subduction zones have been identified. The trough below Uorsar Rupes and its associated rise to the north resemble the flexural trough and outboard rise of terrestrial subduction zones [Solomon and Head, 1990]. Sandwell and Schubert [1992] identify similar trough and rise features forming the outer boundaries of some coronae, and propose their formation though the downward flexure and possible subduction of the surrounding lithosphere under the radially spreading central corona mass, with the flexural load supplied by either the overriding plate or the subducted slab. Further examples include arcuate trenches observed in eastern Aphrodite Terra on Venus and interpreted by McKenzie et al. [1992] to be subduction zones on the basis of their similarity to subduction zones on Earth.

While the role of plate tectonic processes appears minor in the overall evolution of the Venusian lithosphere, underthrusting and subduction potentially contribute to the creation of many observed features. To the extent that the surface tectonic consequences of these two processes would differ, with underthrusting leading primarily to crustal thickening and possible melt production, while the results of subduction may not resemble those found on Earth, the factors governing the dominance of one process over the other are therefore important.

In order to evaluate the conditions distinguishing underthrusting and subduction, we have modelled the thermal and buoyancy consequences of the subduction endmember. This study considers the fate of a slab from the time it starts to subduct, but bypassing the question of subduction initiation. Thermal changes in slabs subducting into a mantle having a range of initial geotherms are used to predict density changes and, thus, slab buoyancy. This then forms part of an argument, utilizing a model for subduction-induced mantle flow, whereby the angle of slab dip helps differentiate between underthrusting and subduction. Mantle flow applies torques to the slab which, in combination with torques due to slab buoyancy, act to change the angle of slab dip.

Subduction Model

In the model (Figure 1), slabs having a thickness set by 90% of the basalt solidus subduct at a fixed angle into the mantle. Geotherms proposed for Venus range from 5°C/km [Sandwell and Schubert, 1992] to 25°C/km [Solomon and Head, 1990]. The initial model geotherms, matching surface thermal gradients of 10°C/km, 15°C/km, and 25°C/km [Hess and Head, 1989], were calculated using the instantaneous cooling of a semi-infinite half space, and cover most of the proposed range. The model permits cooling of the mantle with time, allowing the evolution of initial high geotherms toward the lower end of the range. A basaltic mantle and slab is assumed for the purpose of the thermal evolution calculations

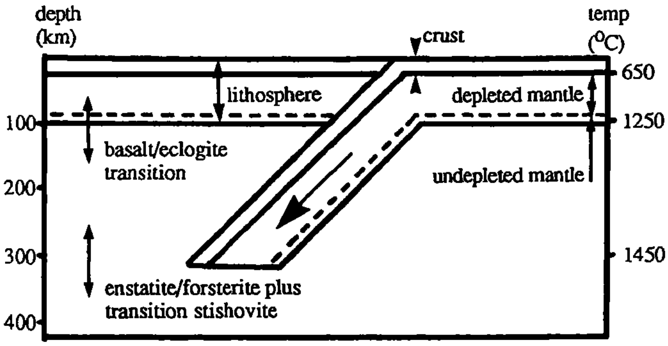

Fig. 1. Model structure for a 10°C/ km geotherm and a 25 km thick basaltic crust.

(basalt and peridotite material properties differ insignificantly in terms of heat conduction). Slabs heat via conduction, radioactivity, phase changes, and adiabatic compression. Phase changes involving the conversion of basalt to eclogite at depths of 60 to 160 km and then enstatite to forsterite plus stishovite between 260 and 360 km generate 0.13×10^{-5} ergs/cm^3-s and 0.36×10^{-5} ergs/cm^3-s respectively [Minear and Toksoz, 1970]. The assumed slab radiogenic heat production is 2.63×10^{-7} ergs/gm-s [Turcotte and Schubert, 1982] while radioactivity in the mantle is considered negligible and ignored. Adiabatic compression adds 0.5°C/km. A dynamic mantle could significantly affect slab temperatures. However, since subducting terrestrial slabs are generally in compression, mantle motion presumably does not keep pace with that of the slab. If a similar situation occurs on Venus, the thermal evolution may more closely resemble the case for an immobile mantle than for one in which the mantle moves with the slab. Therefore, for the purpose of this initial treatment, we neglect the effects of a dynamic mantle in the thermal evolution calculations.

We follow the slab thermal evolution using a finite difference technique [Minear and Toksoz, 1970]. The model region measures approximately 800 km horizontally by 400 km deep. Convergence rates range from 5 to 100 mm/yr and processing ends at the point where slab tips reach a 300 km depth, implying time intervals of 10 to 100 Ma.

Slab density changes derive from the thermal results through calculation of the thermal expansion ($a_V = 3 \times 10^{-5}$ / °K [Stacey, 1977]) and the effects of pressure ($b = 1 \times 10^{-3}$/kb [Turcotte and Schubert, 1982]) on an initial density distribution set for zero pressure and temperature. While the coefficient of thermal expansion changes with temperature and pressure (the value used applies to shallow depths, but a_V decreases to 2×10^{-5} / °K by the base of the model region [Stacey, 1977]), the error introduced by the use of a constant value is on the order of 1%. The assumed initial density structure [Oxburgh and Parmentier, 1977] includes a 10 or 25 km basaltic crust (ρ=3.0 gm/cm^3); a corresponding 25 or 65 km thick depleted mantle zone (ρ=3.295 gm/cm^3); and an underlying undepleted mantle (ρ=3.36 gm/cm^3). The crustal thicknesses were selected to illustrate the effects of changing the crustal thickness, and represent a range proposed for Venus [Zuber, 1987; Grimm and Solomon, 1988], although the exact average thickness is unknown. The initial density structure is based upon the assumption that basaltic crust is derived by the partial melting of the mantle. This creates a low-density depleted mantle layer below the crust [Oxburgh and Parmentier, 1977; Parmentier and Hess, 1992]. We do not mean to imply that crust forms in a ridge-type spreading center. Density changes include those due to phase transitions.

The sample shown in Figure 3 is for a 25 km crust and a 10°C/km initial surface geotherm. The lithosphere includes layers of depleted and undepleted mantle material.

Results

Results of the thermal evolution take the form of temperature distributions in the slab and mantle. The principal effect produced is slab-induced mantle cooling. Figure 2 shows typical results of the density modeling computations, corresponding to the case presented in Figure 1 for a 10°C/km geotherm, 25 km crust, and 5 km/Ma subduction rate. Density contours delineate the slab and its crustal layer. The crust is distinctly lower in density than its surroundings above the 110 km depth assumed for the basalt-eclogite phase change. Below the phase change the crustal material is of greater density than the mantle. The depleted mantle portion of the slab is less clearly delineated and is bounded by the thin undepleted mantle layer included in the lithosphere. The undepleted mantle portion of the slab is denser than the surrounding mantle because of its lower temperature.

The net slab densities in the region above the basalt-eclogite phase transition are lower than their mantle surroundings for every geotherm, subduction rate, and crustal thickness. Above the 110 km depth, crustal densities are lower than those of the mantle outside the slab. The mantle portions of the slab differ slightly in density with mantle outside the slab. Above 110 km depth the crustal portion is much less dense than the mantle slab layers. Below that depth the reverse is true. Below the basalt-eclogite phase change net slab densities always exceed those in the neighboring mantle.

Discussion

Qualitatively, subduction is likely to be enhanced by negative and hindered by positive slab buoyancy. For all geotherms positive net buoyancy persists above the basalt-eclogite phase change. Full length slabs were negatively buoyant in all cases.

We used a model for slab motion-induced mantle flow to evaluate the effects of buoyancy on subduction [Turcotte and Schubert, 1982]. The flow applies a torque to the body of the slab (Figure 3). Mantle dynamics could contribute to the

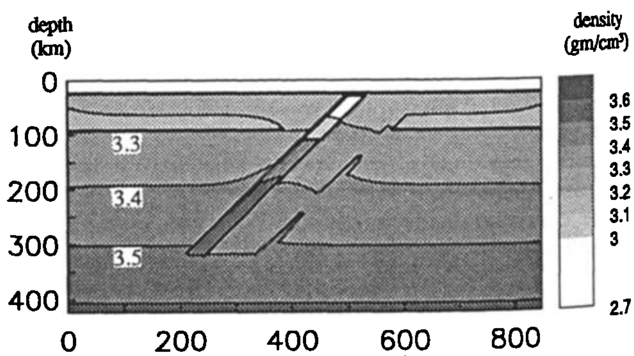

Fig. 2. Final density distribution for 10°C/km initial geotherm, 25 km basaltic crust, and 5 km/Ma subuction rate. Diagram shows contours of density in gm/cm^3, 0.1 gm/cm^3 spacing.

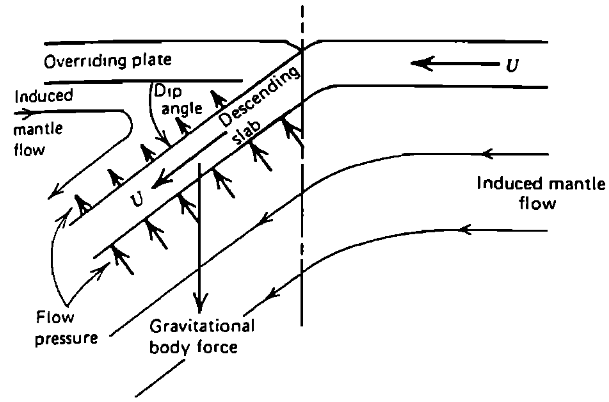

Fig. 3. Diagram of mantle flow induced by slab motion (from Turcotte and Schubert, 1982).

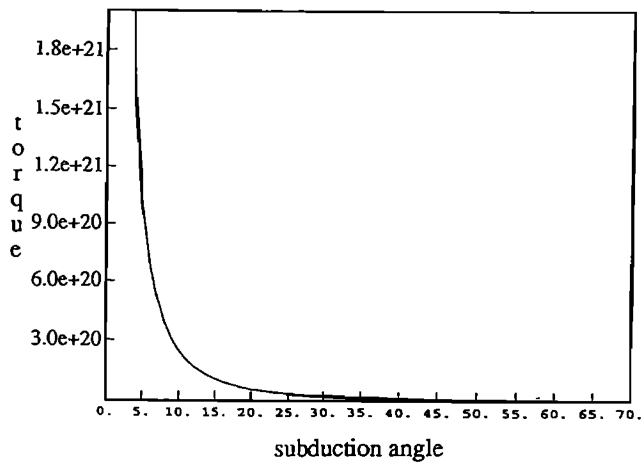

Fig. 4. Torques imposed on the slab by induced mantle flow for a range of subduction angles. Torques are in units of Nm.

torques bearing on the slab, however, the nature of mantle dynamics on Venus is unknown. Mantle flow could be part of a large convective system independent of slab motion. Because of the uncertainty involved in modelling mantle flow, we assume the simplest case of flow due to slab motion. Induced flow depends on assuming a rigid slab. Slab heating will diminish that rigidity, and decrease the calculated flow torques.

Buoyancy body forces also resolve into a torque on the slab, and both torques are taken to act on the slab about its junction with the surface. Table 1 lists buoyancy torques for four subduction rates, both crustal thicknesses, and shallow and full length slabs. Figure 4 plots flow torques versus subduction angle for a 100 km/Ma subduction rate. Flow torques are positive and small (relative to buoyancy torques) for subduction angles over about 15 degrees, becoming large for small angles. Positive torques tend to decrease the subduction angle. For the short slabs dip angles tend to decrease due to both the buoyancy and flow torques. No matter what initial angle a slab would take into a mantle under these conditions, the buoyancy and mantle flow would combine to prevent subduction and underthrusting would result. Further, since the crustal portion of the slab would be positively buoyant, though the mantle part of the slab is negatively buoyant, perhaps delamination could be expected. In this case crustal slices may underthrust and imbricate while the rest of the slab could sink.

For all cases of subduction rate and geotherm the 400 km long slab buoyancy torques are negative and large, exceeding flow torques at angles over 10 degrees. If slabs somehow subduct beyond the neutral buoyancy depth, the negative net buoyancy could help drive subduction. Buoyancy torques for all but the shallowest dip angles are negative and greater than the mantle flow torques, resulting in increased slab dip.

For crustal thicknesses outside of the modelled range, some buoyancy effects may differ. For crust thinner than 10 km, the positive buoyancy resulting from the low crustal and depleted mantle densities would be decreased. The increase of density due to the conversion of basalt to eclogite would also be smaller. Thus, slabs having thin crustal layers would follow the same buoyancy trend as those modelled here, but with a smaller net buoyancy difference. If the crust were about 100 km thick the lithospheric slab may be comprised entirely of crust and depleted mantle, or even entirely crust, depending on the geotherm. The net positive or negative buoyancy of such slabs, above or below the basalt-eclogite transition, respectively, would be more extreme than for thinner crustal layers.

These results indicate that for all cases considered here of assumed Venus geotherm a lithospheric slab whose subduction has been initiated will be forced to underthrust the overriding lithosphere. Also, since the crustal material in a shallow slab is positively buoyant, while the rest of the slab may be

TABLE 1: Torques due to slab buoyancy.

geotherm (°C/km)	subd. rate (km/Ma)	10 km crust buoyancy torque (Nm) 400 km slab	10 km crust buoyancy torque (Nm) 110 km slab	25 km crust buoyancy torque (Nm) 400 km slab	25 km crust buoyancy torque (Nm) 110 km slab
25	100	-1.0×10^{21}	1.5×10^{20}	-2.5×10^{21}	2.8×10^{20}
25	50	-7.1×10^{20}	1.9×10^{20}	-2.2×10^{21}	3.2×10^{20}
25	25	-5.6×10^{20}	2.1×10^{20}	-2.0×10^{21}	3.4×10^{20}
25	5	-3.6×10^{20}	2.5×10^{20}	-1.8×10^{21}	3.8×10^{19}
15	100	-2.6×10^{21}	-1.5×10^{19}	-3.8×10^{21}	4.9×10^{19}
15	50	-2.0×10^{21}	3.9×10^{19}	-3.1×10^{21}	1.0×10^{20}
15	25	-1.7×10^{21}	7.1×10^{19}	-2.8×10^{21}	1.3×10^{20}
15	5	-9.8×10^{20}	1.6×10^{20}	-2.1×10^{21}	2.2×10^{20}
10	100	-3.8×10^{21}	1.2×10^{20}	-3.7×10^{21}	9.1×10^{19}
10	50	-3.1×10^{21}	1.4×10^{20}	-3.1×10^{21}	1.1×10^{20}
10	25	-2.8×10^{21}	1.5×10^{20}	-2.5×10^{21}	2.8×10^{20}
10	5	-2.4×10^{21}	1.6×10^{20}	-2.3×10^{21}	1.3×10^{20}

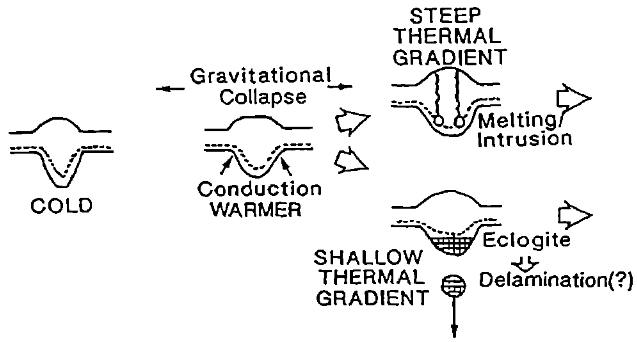

Fig. 5. Possible results of crustal thickening including melting of the crustal root and, alternatively, delamination after root has deepened through the basalt-eclogite phase transition (from Vorder Bruegge and Head, 1991).

negatively buoyant or neutral, some sort of crustal detachment may be possible. These both could then lead to crustal thickening, melting and volcanism, and possibly provide one model to explain the association of compressional mountain belts and blocks of high standing tessera, with apparent flexural rises, foredeeps, and large volumes of volcanic deposits.

Further work is required to constrain the rate at which a slab may rise to assume an underthrusting position after initially subducting. Nevertheless, we expect that where subduction is initiated it will soon evolve into underthrusting. The flexural signature shown by the lithosphere at Freyja Montes [Solomon and Head, 1990] and around coronae such as Artemis and Latona [Sandwell and Schubert, 1992] should thus be due to the loading provided by the overriding lithosphere and not to a negatively buoyant slab.

Except in the case of an underthrusting/subduction event of short duration, perhaps to be expected around a corona, the tendency to convert subduction into underthrusting should lead to the creation of zones of thickened, deformed crust. As thickening continues, and the crustal root is isostatically forced to deeper levels in the upper mantle, heating of crustal material could trigger the formation of magmas derived by crustal remelting (Figure 5). In the anhydrous mantle of Venus such melts might be SiO_2-poor trachytes and phonolites or ferrobasalts [Hess and Head, 1990]. These could extrude as flood volcanics. The volcanics observed atop Itzpapalotl Tessera may be one example of such materials.

If melting does not occur, because of a low geotherm, the root may deepen to the level of the basalt eclogite phase transition (Figure 5). This densification of the deepest portion of the thickened crust may lead to its detachment and descent into the mantle. Such a delamination would clearly create strong tectonic effects as the remaining crust reequilibrates isostatically. If an underthrust lithospheric slab sutures to the crustal root it could be carried along when that root densifies and detaches. This scenario may then lead to self-sustaining subduction as slab-pull provides the driving force.

Acknowledgments. The authors gratefully acknowledge the financial support of the NASA under grant NAGW-1873 to JWH. The paper benefited from discussions with Marc Parmentier and the comments of two anonymous reviewers.

References

Anderson, D.L., Plate tectonics on Venus, Geophys. Res. Lett., 8, 309-311, 1981.

Burt, J.D., and J.W. Head, Venus: Tectonic and volcanic consequences of subduction and underthrusting, Lunar and Planetary Science XXI, 149-150, 1990.

Crumpler, L.S., J.W. Head, and D.B. Campbell, Orogenic belts on Venus, Geology, 14, 1031-1034, 1986.

Grimm, R.E., and S.C. Solomon, Viscous relaxation of impact crater relief on Venus: Constraints on crustal thickness and thermal gradient, J. Geophys. Res., 93, 11,911-11,929, 1988.

Head, J.W., Formation of mountain belts on Venus: Evidence for large-scale convergence, underthrusting, and crustal imbrication in Freyja Montes, Ishtar Terra, Geology, 18, 99-102, 1990.

Hess, P.C. and Head, J.W., (1990), Derivation of primary magmas and melting of crustal materials on Venus: some preliminary petrogenetic observations, Earth, Moon, and Planets, 50/51, p. 57-80.

Hess, P.C., and J.W. Head, Derivation of primary magmas and melting of crustal materials on Venus: some preliminary considerations, Abstracts of the 28th International Geological Congress, 2-55, 1989.

McKenzie, D., P.G. Ford, C. Johnson, B. Parsons, G.H. Pettengill, D. Sandwell, S. Saunders, and S.C. Solomon, Features on Venus generated by plate boundary processes, J. Geophys. Res. in press, 1992.

Minear, J.W., and M.N. Toksoz, Thermal regime of a downgoing slab and the new global tectonics, J. Geophys. Res., 75, no.8, 1397-1419, 1970.

Oxburgh, E.R., and E.M. Parmentier, Compositional and density stratification in oceanic lithosphere - causes and consequences, J. geol. Soc. Lond., 133, 343-355, 1977.

Parmentier, E.M., and P.C. Hess, Chemical differentiation of a convecting planetary interior: Consequences for one-plate planets such as Venus, Lunar and Planetary Science XXIII, 1037-1038, 1992.

Phillips, R.J., and M.C. Malin, The interior of Venus and tectonic implications, in Venus, Hunten, D.M., et al. eds., U. AZ Press, Tucson, 159-214, 1983.

Sandwell, D.T., and G. Schubert, Is the Venusian lithosphere subducting? , Lunar and Planetary Science XXIII, 1209, 1992.

Solomon, S.C., and J.W. Head, Lithospheric flexure beneath the Freyja Montes foredeep, Venus: constraints on lithospheric thermal gradient and heat flow, Geophys. Res. Lettr., 17, no.9, 1393-1396, 1990.

Stacey, F.D., A thermal model of the Earth, Phys. Earth planet. Interiors, 15, 341-348, 1977.

Turcotte, D.L., and G. Schubert, Geodynamics: Applications of Continuum Physics to Geological Problems, J. Wiley & Sons, New York, 450 pp., 1982.

Vorder Bruegge, R.W., and J.W. Head, Fortuna Tessera, Venus: Evidence of horizontal convergence and crustal thickening, Geophys. Res. Lett., 16, no. 7, 699-702, 1989.

Zuber, M.T., Constraints on the lithospheric structure of Venus from mechanical models and tectonic surface features, Proc. Lunar Planet. Sci. Conf. 17th, Part 2., 1987.

J.D. Burt and J.W. Head, Department of Geological Sciences, Box 1846, Brown University, Providence, RI 02912.

(Received May 12, 1992;
accepted June 25, 1992.)